

1 **Rapid and sensitive virulence prediction and identification of Newcastle disease virus**  
2 **genotypes using third-generation sequencing**

3 Salman Latif Butt<sup>a,b</sup>, Tonya L. Taylor<sup>a</sup>, Jeremy D. Volkening<sup>c</sup>, Kiril M. Dimitrov<sup>a</sup>, Dawn  
4 Williams-Coplin<sup>a</sup>, Kevin K. Lahmers<sup>d</sup>, Asif Masood Rana<sup>e</sup>, David L. Suarez<sup>a</sup>, Claudio L. Afonso<sup>a#</sup>,  
5 James B Stanton<sup>b#</sup>.

6 a. Exotic and Emerging Avian Viral Diseases Research Unit, Southeast Poultry Research  
7 Laboratory, US National Poultry Research Center, Agricultural Research Service, USDA, 934  
8 College Station Road, Athens, GA, 30605, USA.

9 b. Department of Pathology, College of Veterinary Medicine, University of Georgia, Athens, GA,  
10 30602, USA.

11 c. BASE2BIO, Oshkosh, WI, USA.

12 d. Department of Biomedical Sciences & Pathobiology, VA-MD College of Veterinary Medicine,  
13 Virginia Tech, VA, USA.

14 e. Hivet Animal Health Business, 667-P, Johar Town, Lahore, Pakistan

15 # Co-corresponding authors:

16

17 **Claudio L. Afonso** Email: [Claudio.Afonso@ars.usda.gov](mailto:Claudio.Afonso@ars.usda.gov)

18 **James B. Stanton** Email: [jbs@uga.edu](mailto:jbs@uga.edu)

19

20 Running title: MinION-based virulence and genotype prediction of NDV

21 **Abstract**

22 Newcastle disease (ND) outbreaks are global challenges to the poultry industry. Effective  
23 management requires rapid identification and virulence prediction of the circulating Newcastle  
24 disease viruses (NDV), the causative agent of ND. However, these diagnostics are hindered by the  
25 genetic diversity and rapid evolution of NDVs. A highly sensitive amplicon sequencing (AmpSeq)  
26 workflow for virulence and genotype prediction of NDV samples using a third-generation, real-  
27 time DNA sequencing platform is described using both egg-propagated virus and clinical samples.  
28 1D MinION sequencing of barcoded NDV amplicons was performed on 33 egg-grown isolates,  
29 (23 unique lineages, including 15 different NDV genotypes), and from 15 clinical swab samples  
30 from field outbreaks. Assembly-based data analysis was performed in a customized, Galaxy-based  
31 AmpSeq workflow. For all egg-grown samples, NDV was detected and virulence and genotype  
32 were predicted. For clinical samples, NDV was detected in ten of eleven NDV samples. Six of the  
33 clinical samples contained two mixed genotypes, of which the MinION method detected both  
34 genotypes in four of those samples. Additionally, testing a dilution series of one NDV sample  
35 resulted in detection of NDV with a 50% egg infectious dose (EID<sub>50</sub>) as low as 10<sup>1</sup> EID<sub>50</sub>/ml. This  
36 was accomplished in as little as 7 minutes of sequencing time, with a 98.37% sequence identity  
37 compared to the expected consensus. The high sensitivity, fast sequencing capabilities, accuracy  
38 of the consensus sequences, and the low cost of multiplexing allowed for identification of NDV  
39 of different genotypes circulating worldwide. This general method will likely be applicable to  
40 other infectious agents.

## 41 **Introduction**

42 Newcastle disease (ND) is one of the most important infectious diseases of poultry and is  
43 a major cause of economic losses to the global poultry industry. Newcastle disease is caused by  
44 virulent strains of avian paramyxovirus 1 (APMV-1), commonly known as Newcastle disease virus  
45 (NDV) (1), recently reclassified as avian avulavirus-1 (AAvV-1) (2). Newcastle disease viruses  
46 are a highly diverse group of viruses with two distinct classes and 19 accepted genotypes, infecting  
47 a wide range of domestic and wild bird species. In addition to the genotypic diversity of NDVs,  
48 these viruses are also diverse in their virulence. The global spread, constant evolution, varying  
49 virulence, and the wide host range of NDV are challenges to the control of ND (3).

50 Effective control of ND is dependent on rapid, sensitive, and specific diagnostic testing,  
51 which for ND are typically oriented towards detection, genotyping, or prediction of virulence.  
52 Virulence of NDV is best assayed through infection-based studies (4), but due to the time  
53 constraints associated with such methods, reverse transcriptase-quantitative PCR (RT-qPCR) and  
54 sequencing of the fusion (F) gene cleavage site are used to predict NDV virulence (5, 6).  
55 Genotyping of NDV is commonly achieved through Sanger sequencing of the coding sequence of  
56 the fusion gene (7), which also allows for prediction of virulence. Preliminary genotyping can be  
57 accomplished through partial fusion gene sequencing (i.e., variable region) (8). PCR-based tests  
58 aimed at rapid detection often lack applicability for virulence determination due to NDV's genetic  
59 diversity, and the current methods that rely on Sanger sequencing lack multiplexing capability and  
60 have limited sequencing depth, which complicates detection of mixed infections. While fusion-  
61 based assays can be used for detection (9), the variability of this region, which makes it useful for  
62 genotyping, hinders the universal applicability of any single primer set. Thus, detection-focused  
63 assays are often designed towards more conserved regions, such as the matrix or polymerase

64 genes(9-11). These assays, however, fail to provide virulence or genotype predictions. In  
65 summary, there is a need for a method that will sensitively and rapidly detect numerous genotypes  
66 of NDV and provide genotype and virulence prediction.

67         Rapid advances in nucleic acid sequencing, have led to different sequencing platforms (12,  
68 13) being widely applied for identification of novel viruses (14), whole genome sequencing (15),  
69 transcriptomics, and metagenomics (16, 17). However, high capital investments and relatively long  
70 turnaround times limit the widespread use of these NGS platforms, especially in developing  
71 countries (18). Recent improvements in third-generation sequencing, including those introduced  
72 by Oxford Nanopore Technologies (ONT) (19), increase the utility of high-throughput sequencing  
73 as a useful tool for surveillance and pathogen characterization (20). Among the transformative  
74 advantages of ONT's sequencing technology are the ability to perform real-time sequence analysis  
75 with a short turnaround time (21), the portability of the MinION device, the low startup cost  
76 compared to other high-throughput platforms, and the ability to sequence up to several thousand  
77 bases from individual RNA or DNA molecules. The MinION device has been successfully used  
78 to evaluate antibiotic resistance genes from several bacterial species (22, 23), obtain complete viral  
79 genome sequences of an influenza virus (24) and Ebola virus (25), and detect partial viral genome  
80 sequences (e.g., Zika virus (26) and poxviruses (21)) by sequencing PCR amplicons (AmpSeq).  
81 The MinION, therefore, represents an opportunity to take infectious disease diagnostics a step  
82 further and to perform rapid identification and genetic characterization of infectious agents at a  
83 lower cost.

84         As with any deep sequencing platform, the sequence analysis approach is integral for  
85 accurate interpretation. Primarily, two approaches for taxonomic profiling of microbial sequencing  
86 data have been employed: read-based and *de novo* assembly-based classifications. Read-based

87 metagenomic classification software has been used for identification of microbial species from  
88 high-throughput sequencing data (19, 27-29). Although the sequencing accuracy of the MinION  
89 is improving, the raw single-read error rate of nearly 10% (30) may limit the accuracy of this  
90 approach for Nanopore data (27), especially when attempting to subspecies level differentiation.  
91 *De novo* approaches that use quality-based filtering and clustering of reads (31), or use consensus-  
92 based error correction of Nanopore sequencing reads have been reported (32); however, these are  
93 not optimized for amplicon sequencing data.

94         In this study, a specific, sensitive, rapid protocol, using the MinION sequencer, was  
95 developed to detect representative isolates from all current (excluding the Madagascar-limited  
96 genotype XI) genotypes of NDV. This protocol was also tested on a limited number of clinical  
97 swab samples collected from chickens during disease outbreaks. Additionally, a Galaxy-based, *de*  
98 *novo* AmpSeq workflow is presented that efficiently reduces systematic sequencing errors in  
99 Nanopore sequencing data and uses amplicon-based sequences to obtain accurate final consensus  
100 sequences.

101

## 102 **Materials and Methods**

### 103 **Viruses**

104 Thirty-three NDV isolates, representing 23 unique lineages (including 15 different  
105 genotypes) of different virulence, and 10 other avian avulaviruses (AAvV 2-10 and AAvV-13)  
106 from the Southeast Poultry Research Laboratory (SEPR) repository, were propagated in 9–11-  
107 day-old specific pathogen free (SPF) eggs (33) and the harvested allantoic fluids were used in this  
108 study. Additionally, 15 oral and cloacal swab samples collected from chickens during disease  
109 outbreaks in Pakistan in 2015 were tested. The background information of the egg-grown isolates  
110 and the clinical samples is summarized in Table S1 and Table S2, respectively.

### 111 **RNA Isolation**

112 Total RNA from each sample was extracted from infectious allantoic fluids or directly from  
113 clinical swab media using TRIzol LS (Thermo Fisher Scientific, USA) following the  
114 manufacturer's instructions. RNA concentrations were determined by using Qubit® RNA HS  
115 Assay Kit on a Qubit® fluorometer 3.0 (Thermo Fisher Scientific, USA).

### 116 **Amplicon synthesis**

117 Approximately 20 ng (in 5 µl) of RNA was reverse transcribed, and cDNA was amplified  
118 with target-specific primers using the SuperScript™ III One-Step RT-PCR System (Thermo Fisher  
119 Scientific, USA). Previously published primers (4331F and 5090R) (8, 34) were used in this  
120 protocol; however, primers were tailed with universal adapter sequence of 22 nucleotides (in bold  
121 font) to facilitate PCR-based barcoding: 4331F Tailed: 5'-  
122 **TTTCTGTTGGTGCTGATATTGCGAGGTTACCTCYACYAAGCTRGAGA**-3'; 5090R  
123 Tailed: 5'-  
124 **ACTTGCCTGTCGCTCTATCTTCTCATTAACAAAYTGCTGCATCTTCCCWAC**-3'). The

125 thermocycler conditions for the reaction were as follows: 50 °C for 30 minutes; 94 °C for 2  
126 minutes; 40 cycles of 94 °C for 15 seconds, 56 °C for 30 seconds, and 68 °C for 60 seconds,  
127 followed by 68 °C for 5 minutes. The reaction amplified a 788 base pair (bp) NDV product (832  
128 bp including primer tails) for all genotypes, which included 173 bp of the 3' region of the end of  
129 the M gene and 615 bp of the 5' end of the F gene (sizes and primer locations based on the Genotype  
130 V strain).

### 131 **Library preparation**

132         Amplified DNA was purified by Agencourt AMPure XP beads (Beckman Coulter, USA)  
133 at 1.6:1 bead-to-DNA ratio and quantified using the dsDNA High Sensitivity Assay kit on a  
134 Qubit® fluorometer 3.0 (Thermo Fisher Scientific, USA). MinION-compatible DNA libraries  
135 were prepared with approximately 1 µg of barcoded DNA in a total volume of 45 µL using  
136 nuclease-free water and using the 1D PCR Barcoding Amplicon Kit (Oxford Nanopore  
137 Technologies, UK) in conjunction with the Ligation Sequencing Kit 1D (SQK-LSK108) (19) as  
138 per manufacturer's instructions. Briefly, each of the amplicons were diluted to 0.5 nM for  
139 barcoding and amplified using LongAmp Taq 2X Master Mix (New England Biolabs, USA) with  
140 the following conditions; 95 °C for 3 min; 15 cycles of 95 °C for 15 seconds; 62 °C for 15 seconds,  
141 65 °C for 50 seconds, followed by 65 °C for 50 seconds. The barcoded amplicons were bead  
142 purified, pooled into a single tube, end prepped, dA tailed, bead purified, and ligated to the  
143 sequencing adapters per manufacturer's instructions. Final DNA libraries were bead purified and  
144 stored frozen until used for sequencing.

### 145 **Comparison to RT-qPCR assay for Matrix gene**

146         For comparison of this MinION-based protocol with the matrix gene reverse transcriptase-  
147 quantitative polymerase chain reaction (RT-qPCR) assay, both methods were run on a dilution

148 series from a single isolate. NDV (LaSota strain) from the SEPRL repository was cultured in SPF  
149 9–11-days-old eggs and the harvested allantoic fluids were diluted to titers ranging from  $10^6$  to  $10^1$   
150  $EID_{50}/mL$  in brain-heart infusion broth. RNA was extracted from dilutions, and DNA libraries  
151 were prepared following the same protocols as described above. Amplicons from each of the  
152 dilutions were barcoded separately. At the pooling step, equal concentrations of barcoded  
153 amplicons from different dilutions of LaSota were pooled together in single tube. Dilutions,  
154 extractions, library construction, and sequencing were performed twice.

155 The same extracted RNA was also used as the input into the RT-qPCR using the AgPath-  
156 ID one-step RT-PCR Kit (Ambion, USA) on the ABI 7500 Fast Real-Time PCR system following  
157 the previously described protocols (9).

#### 158 **Sequencing by MinION**

159 The libraries were sequenced with the MinION Nanopore sequencer (19). A new FLO-  
160 MIN106 R9.4 flow cell, stored at  $4^{\circ}C$  prior to use, was allowed to equilibrate to room temperature  
161 for 10 minutes before priming it for sequencing. The flow cell was primed with running buffer as  
162 per manufacturer's instructions. The pooled DNA libraries were prepared by combining 12  $\mu L$  of  
163 the libraries with 2.5  $\mu L$  nuclease-free water, 35  $\mu L$  RBF, and 25.5  $\mu L$  library loading beads. After  
164 the MinION Platform QC run, the DNA library was loaded into the MinION flow cell via the  
165 SpotON port. The standard 48-h 1D sequencing protocol was initiated using the MinKNOW  
166 software v.5.12. Detailed information for all MinION runs in this study is provided in Table S3.

167 The complete steps from RNA isolation to MinION sequencing were performed twice for  
168 egg-grown viruses. One run consisted of six egg-grown isolates from different genotypes  
169 representative of vaccine and virulent NDV strains (run 3: 6-sample pool). The other run consisted  
170 of these same six viruses and an additional 27 egg-grown NDV isolates (run 4: 33-sample pool).



171 To determine the accuracy of consensus sequences at different sequencing time points for  
172 accurate identification of the NDV genotypes, the raw data (FAST5 files) obtained from the 10-  
173 fold serial dilution experiment (see above) were analyzed in subgroups based on time of  
174 acquisition and processed through the AmpSeq workflow as described below.

### 175 **MinION data analysis workflow**

176 To analyze the Nanopore sequencing data, a custom, assembly-based AmpSeq workflow  
177 within the Galaxy platform interface (35) was developed, as diagrammed in Figure 1. The MinION  
178 raw reads in FAST5 format were uploaded into Galaxy workflow. The reads were base-called  
179 using the Albacore v2.02 (ONT). The NanoporeQC tool v0.001 (available in the Galaxy testing  
180 toolshed) was used to visualize read quality based on the summary table produced by Albacore.  
181 Porechop v0.2.2 (<https://github.com/rrwick/Porechop>) was used to demultiplex reads for each of  
182 the barcodes and trim the adapters at the ends of the reads by using default settings. Short reads  
183 (cutoff = 600 bp) were filtered out and the remaining reads were used as input to the in-house  
184 LAclust v0.002. LAclust performs single-linkage clustering of noisy reads based on alignment  
185 identity and length cutoffs from DALIGNER pairwise alignments (36) (minimum alignment  
186 coverage = 0.90, maximum identity difference = 0.35; minimum number of reads to save cluster  
187 = 5; maximum reads saved per cluster = 200, minimum read length = 600 bp; rank mode = number  
188 of intracluster linkages; randomized input read order = yes). Read clusters generated by LAclust  
189 were then aligned using the in-house Amplicon aligner v0.001 to generate a consensus sequence.  
190 This tool optionally subsamples reads (target depth used = 100), re-orientes them as necessary,  
191 aligns them using Multiple Alignment using Fast Fourier Transform (MAFFT) (37) with highly  
192 relaxed gap opening and extension penalties, and calls a majority consensus. Next, each consensus  
193 was used as a reference sequence for mapping the full unfiltered read clusters from LAclust with

194 BWA-MEM and ONT2D settings (38, 39). The final consensus sequence for each sample was  
195 refined by using Nanopolish v0.8.5 (<https://github.com/jts/nanopolish>), which calculates an  
196 improved consensus using the read alignments and raw signal information from the original  
197 FAST5 files. After manually trimming primer sequences from both 3' (25 bp) and 5' (29 bp) ends,  
198 the obtained consensus sequences (734 bp) were BLAST searched against NDV customized  
199 database, which consisted NCBI's nucleotide (nt) database and internal unpublished NDV  
200 sequences (NCBI database updated on May 23, 2018).

### 201 **Sequencing by MiSeq**

202 For comparison between nucleotide sequences obtained from MinION and MiSeq (a  
203 validated and high accuracy sequencing platform), 24 NDV isolates from the SEPRL repository  
204 that were used for MinION sequencing (representing each genotype and sub-genotype of NDV)  
205 and 15 clinical swab samples (allantoic fluid of cultured swab samples) were processed for target-  
206 independent NGS sequencing. Briefly, paired-end random sequencing was conducted from cDNA  
207 libraries prepared from total RNA using KAPA Stranded RNA-Seq kit (KAPA Biosystems, USA)  
208 as per manufacturer's instructions and as previously described (40). All libraries for NGS were  
209 loaded into the 300-cycle MiSeq Reagent Kit v2 (Illumina, USA) and pair-end sequencing ( $2 \times$   
210 150 bp) was performed on the Illumina MiSeq instrument (Illumina, USA). Pre-processing and  
211 de-novo assembly of the raw sequencing data was completed within the Galaxy platform using a  
212 previously described approach (15).

### 213 **Phylogenetic analysis**

214 The assembled consensus sequences from different NDV genotypes and sub-genotypes (6  
215 sequences from MinION run 3, 32 sequences from run 4 and 24 sequences from MiSeq; a total of  
216 62 sequences) and selected (minimum of one sequence from each genotype/subgenotype)

217 sequences from GenBank (n = 66) were aligned using ClustalW (41) in MEGA6 (42).  
218 Determination of the best-fit substitution model was performed using MEGA6, and the goodness-  
219 of-fit for each model was measured by corrected Akaike information criterion (AICc) and  
220 Bayesian information criterion (BIC) (42). The final tree was constructed using the maximum-  
221 likelihood method based on the General Time Reversible model as implemented in MEGA6, with  
222 500 bootstrap replicates (43). The available GenBank accession number for each sequence in the  
223 phylogenetic tree is followed by the, host name, country of isolation, strain designation, and year  
224 of isolation.

### 225 **Comparison of MinION and MiSeq sequence accuracy**

226 To assess the accuracy of the MinION AmpSeq consensus sequences, 24 samples were  
227 sequenced by both deep-sequencing methods (MinION and MiSeq) described above. Pairwise  
228 nucleotide comparison between MinION and MiSeq was conducted using the Maximum  
229 Composite Likelihood model (44). The variation rate among sites was modeled with a gamma  
230 distribution (shape parameter = 1). The analysis involved 54 nucleotide sequences. Codon  
231 positions included were 1st+2nd+3rd+Noncoding. All positions containing gaps and missing data  
232 were eliminated. There were a total of 691 positions in the final dataset. The evolutionary distances  
233 were inferred by pairwise analysis using the MEGA6 (42).

### 234 **Accession number**

235 The sequences obtained in the current study were submitted to GenBank and are available under  
236 the accession numbers from MH392212 to MH392228.

237

## 238 **Results**

### 239 **Comparison to the Matrix gene RT-qPCR assay**

240 Six, sequential, 10-fold dilutions (from  $10^6$  EID<sub>50</sub>/ml to  $10^1$  EID<sub>50</sub>/ml) from one NDV  
241 isolate (LaSota) were used to compare the ability of AmpSeq and RT-qPCR to detect low  
242 quantities of NDV. In each of the six dilutions, AmpSeq and the matrix RT-qPCR detected NDV  
243 in all dilutions. AmpSeq resulted in 99.04–100.0% sequence identity to the LaSota isolate across  
244 all six dilutions in the first experiment (R1) and 99.86–100.0% identity in the second experiment  
245 (R2) (Table 1).

### 246 **Time for data acquisition and analysis**

247 To determine the minimal sequencing time needed for acquisition of accurate full-length  
248 amplicon consensus sequences at different serial dilutions, 28,000 reads, which were obtained  
249 within the first 19 minutes of sequencing in the first serial dilution experiment (run 1), were  
250 analyzed. For all concentrations, the first read that aligned to the reference LaSota sequence was  
251 obtained within 5 minutes after the sequencing run started. To obtain consensus sequences (5 reads  
252 required to build a consensus sequence) only 5 minutes of sequencing time were required for  
253 concentrations  $10^6$ – $10^3$  EID<sub>50</sub>/ml, which resulted in 99.18–100% sequence identity to the reference  
254 LaSota strain. Seven minutes were required to obtain NDV consensus sequences for the two lower  
255 concentrations:  $10^1$  EID<sub>50</sub>/ml = 8 reads, 98.77% identity and  $10^2$  EID<sub>50</sub>/ml = 5 reads, 98.37%  
256 identity (Table 2).

### 257 **PCR specificity and range of reactivity for NDV genotypes**

258 To determine the utility of the primers for the currently circulating NDV genotypes and the  
259 potential cross-reactivity for other AAVVs, which are relatively nonpathogenic in poultry but can  
260 confound diagnosis of NDV (45), total RNA from 43 AAVVs, including 23 unique AAVV-1

261 lineages, (15 different NDV genotypes, 8 different subgenotypes, total samples = 33), as well as  
262 AAvV-2-10 and -13 (n = 10) were tested. All AAvV-1 genotypes that are currently circulating  
263 globally were amplified with tailed primers; samples 19 and 36 had weak bands of the desired  
264 molecular weight compared to other lanes; samples 19, 20, 21, 31 and 32 had an additional, heavier  
265 band (~1000 bp). All non-AAvV-1 viruses were negative (Figure S1).

## 266 **Quality metrics**

267 The Nanopore QC tool was used to obtain quality metrics plots of all sequencing runs. For  
268 MinION runs 3 (6 multiplexed samples) and 4 (33 multiplexed samples), more than 70% of total  
269 reads had a quality score greater than ten (Q10 score = 90% accuracy) (Figure S2 A and B). The  
270 average overall mean read quality scores in both runs were comparable (run 3 = 10.7, run 4 = 11.0),  
271 and the mean quality scores of reads  $\geq 10$  (mean  $Q_{\geq 10}$ ) were similar (11.8) for both runs (Figure S2).  
272 In addition, analysis of five consecutive batches of reads (each batch = 20,000 reads) obtained at  
273 different time intervals from run 4 indicated that the overall mean read quality for each 20,000 read  
274 batch remained above 10 (Table S4). Similarly, the mean  $Q_{\geq 10}$  over time remained consistent in the  
275 clinical sample runs (runs 5–7), which had long (12 hrs) sequencing runs (Figure S3, green lines).

## 276 **Sub-genotypic resolution of AAvV-1 viruses with MinION sequencing**

277 To determine the capability to effectively detect and differentiate viruses of different  
278 genotypes, PCR amplicons from 33 egg-gown isolates, which were representative of 23 different  
279 NDV lineages including 15 different genotypes, were barcoded, pooled, and sequenced in a single  
280 12-hour MinION run (run = 4) generating a total of 2.076 million reads. The first 100,000 reads,  
281 which were obtained in 3 hours and 10 minutes, were analyzed for identification of all 33 NDV  
282 isolates used in the study. All 33 NDV isolates were correctly identified to the sub-genotype level

283 (Table 3). These consensus sequences had 97.82–100% sequence identity to the expected sequence  
284 in each of the samples.

285 While 788 bp was the expected amplicon size, genotypes III, IV, and IX (all previously  
286 untested genotypes with this primer set) yielded an unexpected electrophoresis product of ~1000  
287 bp (see above). The sequences obtained from these NDV isolates revealed that in addition to the  
288 788 bp product, an upstream region of NDV genome was amplified, resulting in 1050 bp consensus  
289 sequences.

290 Two virus isolates contained two NDV genotypes. For sample #37, MiSeq detected  
291 genotypes XIIIb and VIc, but the AmpSeq workflow only detected genotype XIIIb. Sample #16  
292 had been previously confirmed to contain two genotypes, as determined by two genotype-specific  
293 PCRs and Sanger sequencing (data not shown); however, the MinION-based AmpSeq workflow  
294 only detected genotype VIIId.

### 295 **Clinical swab samples from chicken**

296 To assess the potential utility of the protocol on clinical field samples, MinION libraries  
297 were generated directly from clinical swab samples. Also, for confirmation, these swab samples  
298 were cultured in eggs and the allantoic fluid was sequenced using a MiSeq-based workflow. Out  
299 of 11 NDV-positive samples with the culture-MiSeq method, 10 samples were NDV positive by  
300 the MinION protocol (Sample #52 being the exception) (Table 4). In the six NDV-positive samples  
301 that contained one NDV genotype, as detected by the culture-MiSeq method, the same NDV  
302 genotype was also detected with the MinION protocol. The culture-MiSeq method detected two  
303 genotypes in samples #45, #46, #47, and #49; whereas, the MinION protocol only detected dual  
304 genotypes in samples #45 and #46. In sample #48, only one NDV genotype was detected by

305 culture-MiSeq but two NDV genotypes were detected by the MinION protocol. All 4 samples  
306 negative by culture-MiSeq were also negative by the MinION protocol.

### 307 **Pairwise comparison of replicated MinION sequences and MiSeq sequences**

308 Pairwise nucleotide distance analysis was used to compare the consensus sequences in six  
309 samples across two separate MinION runs, and to compare the MinION consensus sequence to the  
310 MiSeq consensus sequence in twenty-four isolates (one isolate representing each genotypes and  
311 sub-genotype). There was no variation in the consensus sequence between the MinION runs across  
312 those six samples. The MinION and MiSeq consensus sequences were 100% identical, except for  
313 sample #37 where the sequence identity was 99.99% to the paired MiSeq sequence. Collectively,  
314 these results demonstrate the repeatable accuracy of the MinION-AmpSeq method.

### 315 **Phylogeny of NDV genotypes**

316 To confirm the ability of the MinION-acquired partial matrix and fusion gene sequences  
317 to be used for accurate analysis of evolutionary relatedness, phylogenetic analysis using consensus  
318 sequences (734 bp) obtained from two independent MinION runs (run 3 and 4) was performed.  
319 Additionally, the 24 sequences from MiSeq were also included in the phylogenetic tree (Figure 2)  
320 to further illustrate the agreement between these two sequencing methods. In the phylogenetic tree,  
321 the isolates (n = 33; green font) grouped together with the viruses that showed highest nucleotide  
322 sequence identity to them, including those in which MiSeq sequences were available (red font).  
323 The six isolates that were sequenced twice (blue font) clustered together. Taken together, the  
324 results demonstrated that all sequences clustered to the expected genotype/sub-genotype branch of  
325 the phylogram.

### 326 **Time and cost estimation**

327           The time of sample processing and cost estimation of reagents to multiplex and sequence  
328 samples ( $n = 6$ ;  $n = 33$ ) from RNA extraction to obtain final consensus sequences is presented in  
329 Table S5. From RNA extraction to final consensus sequence calculations, the average time  
330 (including sequencing time) to process six samples was approximately 9–10 person-hours and for  
331 33 samples approximately 26 person-hours. Assuming that flow cell can be used multiple times  
332 (twice when 33 samples pooled and five times when six samples pooled to prepare one cDNA  
333 library) for sequencing, cost per sequencing run and cost per sample were calculated. The cost per  
334 sample decreased from \$53 (six samples multiplexed) to \$31 (33 samples multiplexed).



## 335 **Discussion**

336           This study describes a sequencing protocol for rapid and accurate detection, virulence  
337 determination, and preliminary genotype identification (with sub-genotype resolution) of NDV  
338 utilizing the low-cost MinION sequencer. Additionally, an assembly-based sequence analysis  
339 workflow is described for analyzing MinION amplicon sequencing data. This MinION AmpSeq  
340 workflow was successful when using a lab repository of egg-grown viruses of varying genotypes,  
341 clinical swab samples, and samples containing mixed genotypes.

342           The sequence heterogeneity among AAvV-1 genomes is well known (3, 46, 47), which  
343 complicates the ability to develop a single test that sensitively detects NDV, while also predicting  
344 the genotypic classification and virulence. Currently, an RT-qPCR targeting the M gene (9) is most  
345 sensitive and is used for screening samples, but this assay only provides positive and negative  
346 results of the samples. An RT-qPCR that predicts virulence based on the fusion gene is available  
347 (9); however, the lower sensitivity of this assay and the inability of this assay to detect all  
348 genotypes (e.g., genotypes Va and VI) (9, 10, 48) complicate diagnostic interpretation when the  
349 matrix and fusion tests have conflicting results. Thus, the only truly reliable option to detect some  
350 viruses is to design genotype-specific primers and probes (6, 48, 49). For example, Miller *et al*  
351 reported that the primer set used in this study detected Class I and all nine of the tested class II  
352 genotypes (34); however, this primer set was not tested against other currently circulating  
353 genotypes, nor was the sensitivity well defined. The current study includes six additional  
354 genotypes, collectively representing all currently circulating genotypes (excluding the  
355 Madagascar-limited genotype XI). Additionally, while the preliminary analytical sensitivity of this  
356 protocol was determined using only one NDV genotype, the sensitivity of the MinION AmpSeq  
357 was comparable to the matrix RT-qPCR and presents an opportunity to implement detection,

358 genotype prediction, and virulence prediction into a single test. As an example of this, in several  
359 clinical samples the MinION AmpSeq method detected and identified the LaSota vaccine strain,  
360 which is an extensively used vaccine strain for commercial poultry in this region (50). Whereas  
361 with the matrix RT-qPCR, these samples would have only been reported as NDV positive and  
362 would have required additional testing to determine that the NDV was not virulent.

363         While the multifaceted nature of this MinION AmpSeq protocol is an advantage, cost and  
364 time efficiency must be maintained for it to be useful outside of research laboratories. MinION is  
365 inherently rapid due to the real-time nature of the sequencing. Additionally, samples can be  
366 multiplexed into a single sequencing run, which reduces time and cost (51). Recently, multiplexing  
367 and MinION sequencing of the PCR products from a panel of 5 samples was reported (51). Here  
368 a panel of 33 samples was multiplexed while maintaining successful NDV genotyping from data  
369 collected within 3 hrs and 10 minutes of sequencing and without affecting mean read quality and  
370 percentage of high quality reads.

371         While Nanopore sequencing has numerous benefits useful for diagnostic testing, the high  
372 error rate poses unique challenges to data analysis. Thus, it is important to extract accurate  
373 consensus sequences from raw sequencing data (52). As previously discussed, pathogen typing  
374 from sequencing data can be done with read count-based profiling or *de novo* assembly approaches  
375 (27). However, there are a limited number of available tools suitable for handling the noisy reads  
376 currently produced by the MinION platform. The approach in this study takes advantage of the  
377 fact that single MinION reads often represent full-length amplicon sequences. By clustering full-  
378 length reads based on pairwise identity and subsequently performing consensus calling using  
379 standard multiple alignment software, this method quickly and reliably generates accurate *do novo*  
380 assemblies from amplicon datasets. Additional refinement using the Nanopolish finisher leads to

381 reliable consensus accuracy >99% with as few as twenty reads per amplicon, and correct genotypic  
382 assignments with as few as five reads per amplicon. Thus, this method overcomes the inherently  
383 high error rate of Nanopore sequencing and sequence identification and differentiation at the sub-  
384 genotype level can be highly reliable.

385         Because this protocol relies on identity-based clustering prior to assembly, it maintains the  
386 ability to detect samples with mixed NDV genotypes, similar to read-based analytical methods.  
387 For example, in this study four clinical samples had two different genotypes as detected by MiSeq  
388 analysis, two of which were correctly identified by the MinION AmpSeq workflow. In a fifth case,  
389 a mixed sample was detected by MinION AmpSeq, but not by MiSeq. A potential explanation for  
390 these differences could be that the MiSeq sequencing was performed on egg-amplified samples,  
391 which may have altered the relative levels of the two genotypes, as compared to the direct clinical  
392 swab sample used for MinION sequencing. Additionally, the differences in molecular techniques  
393 (i.e., MinION: targeted; MiSeq: random) may have altered the relative abundance of the genotypes  
394 within the sequencing libraries. While further studies into the ability of this workflow to detect  
395 and differentiate NDV in samples with more than one genotype are ongoing, rapid NDV  
396 genotyping from clinical samples without culturing the virus in SPF eggs has the potential to  
397 facilitate disease diagnostics.

398         Taken together, this protocol reliably detected, genotyped, and predicted the virulence of  
399 NDV. A MinION AmpSeq-based approach will be beneficial worldwide and especially in  
400 developing countries where the endemicity of high-consequence diseases, such as NDV, and lack  
401 of resources are additional challenges to monitoring and studying infectious diseases (50).  
402 Furthermore, the advantages of MinION AmpSeq allow for further optimization not possible with  
403 other techniques. For example, PCR product length is less of a restriction with MinION AmpSeq

404 as compared to RT-qPCR; thus, there will be one less restriction on primer site design when trying  
405 to create a pan-NDV primer set. Work is in progress to utilize the ability of MinION to sequence  
406 longer amplicon fragments, which will provide more complete phylogenetic information and may  
407 improve the sensitivity of this assay. Overall, MinION AmpSeq improves the depth of information  
408 obtained from PCRs and allows for more flexibility in assay design, which can be broadly applied  
409 to the detection and characterization of numerous infectious agents.

#### 410 **Acknowledgments**

411 We gratefully acknowledge Tim Olivier for technical assistance. Special thanks to the  
412 Fulbright U.S. Student Program for sponsoring Dr. Salman's PhD research work. This project was  
413 supported by USDA CRIS 6040-32000-072 and DTRA grant 58.0210.5.006 and partially funded  
414 by BAA# FRCALL 12-6-2-0015.

## 415 References

- 416
- 417 1. Miller PJ, Koch G. 2013. Newcastle disease. *Diseases of Poultry*, 13th ed(Swayne, DE, Glisson, JR,  
418 McDougald, LR, Nolan, LK, Suarez, DL and Nair, VL eds), John Wilkey and Sons, Inc, Ames:89-107.
  - 419 2. Amarasinghe GK, Ceballos NGA, Banyard AC, Basler CF, Bavari S, Bennett AJ, Blasdel KR, Briese  
420 T, Bukreyev A, Cai Y. 2018. Taxonomy of the order Mononegavirales: update 2018. *Arch Virol*:1-12.
  - 421 3. Dimitrov KM, Ramey AM, Qiu X, Bahl J, Afonso CL. 2016. Temporal, geographic, and host  
422 distribution of avian paramyxovirus 1 (Newcastle disease virus). *Infect Genet Evol* 39:22-34.
  - 423 4. Commission IOoEBS, Committee IOoEI. 2008. Manual of diagnostic tests and vaccines for terrestrial  
424 animals: mammals, birds and bees, vol 2. Office international des épizooties.
  - 425 5. Aldous E, Mynn J, Banks J, Alexander D. 2003. A molecular epidemiological study of avian  
426 paramyxovirus type 1 (Newcastle disease virus) isolates by phylogenetic analysis of a partial  
427 nucleotide sequence of the fusion protein gene. *Avian Pathol* 32:237-255.
  - 428 6. Kim LM, King DJ, Guzman H, Tesh RB, da Rosa APT, Bueno R, Dennett JA, Afonso CL. 2008.  
429 Biological and phylogenetic characterization of pigeon paramyxovirus serotype 1 circulating in wild  
430 North American pigeons and doves. *J Clin Microbiol* 46:3303-3310.
  - 431 7. Diel DG, da Silva LH, Liu H, Wang Z, Miller PJ, Afonso CL. 2012. Genetic diversity of avian  
432 paramyxovirus type 1: proposal for a unified nomenclature and classification system of Newcastle  
433 disease virus genotypes. *Infect Genet Evol* 12:1770-1779.
  - 434 8. Kim LM, King DJ, Suarez DL, Wong CW, Afonso CL. 2007. Characterization of class I Newcastle  
435 disease virus isolates from Hong Kong live bird markets and detection using real-time reverse  
436 transcription-PCR. *J Clin Microbiol* 45:1310-1314.
  - 437 9. Wise MG, Suarez DL, Seal BS, Pedersen JC, Senne DA, King DJ, Kapczynski DR, Spackman E.  
438 2004. Development of a real-time reverse-transcription PCR for detection of newcastle disease virus  
439 RNA in clinical samples. *J Clin Microbiol* 42:329-338.
  - 440 10. Kim LM, Suarez DL, Afonso CL. 2008. Detection of a broad range of class I and II Newcastle  
441 disease viruses using a multiplex real-time reverse transcription polymerase chain reaction assay. *J Vet*  
442 *Diagn Invest* 20:414-425.
  - 443 11. Fuller CM, Brodd L, Irvine RM, Alexander DJ, Aldous EW. 2010. Development of an L gene real-  
444 time reverse-transcription PCR assay for the detection of avian paramyxovirus type 1 RNA in clinical  
445 samples. *Arch Virol* 155:817-23.
  - 446 12. Ambardar S, Gupta R, Trakroo D, Lal R, Vakhlu J. 2016. High Throughput Sequencing: An  
447 Overview of Sequencing Chemistry. *Indian J Microbiol* 56:394-404.
  - 448 13. Rhoads A, Au KF. 2015. PacBio sequencing and its applications. *Genomics Proteomics*  
449 *Bioinformatics* 13:278-289.
  - 450 14. Chiu CY. 2013. Viral pathogen discovery. *Curr Opin Microbiol* 16:468-478.
  - 451 15. Dimitrov KM, Sharma P, Volkening JD, Goraichuk IV, Wajid A, Rehmani SF, Basharat A, Shittu I,  
452 Joannis TM, Miller PJ, Afonso CL. 2017. A robust and cost-effective approach to sequence and  
453 analyze complete genomes of small RNA viruses. *Virol J* 14:72.
  - 454 16. Cruz-Rivera M, Forbi JC, Yamasaki L, Vazquez-Chacon CA, Martinez-Guarneros A, Carpio-Pedroza  
455 JC, Escobar-Gutiérrez A, Ruiz-Tovar K, Fonseca-Coronado S, Vaughan G. 2013. Molecular  
456 epidemiology of viral diseases in the era of next generation sequencing. *J Clin Virol* 57:378-380.
  - 457 17. Marston DA, McElhinney LM, Ellis RJ, Horton DL, Wise EL, Leech SL, David D, de Lamballerie X,  
458 Fooks AR. 2013. Next generation sequencing of viral RNA genomes. *BMC Genomics* 14:444.
  - 459 18. Gullapalli RR, Desai KV, Santana-Santos L, Kant JA, Becich MJ. 2012. Next generation sequencing  
460 in clinical medicine: Challenges and lessons for pathology and biomedical informatics. *J Pathol Inform*  
461 3:40.
  - 462 19. Phan H, Stoesser N, Maciucă I, Toma F, Szekely E, Flonta M, Hubbard A, Pankhurst L, Do T, Peto T.  
463 2017. Illumina short-read and MinION long-read whole genome sequencing to characterise the

- 464       molecular epidemiology of an NDM-1-*Serratia marcescens* outbreak in Romania. *J Antimicrob*  
465       *Chemother* 73 (3) 672–679.
- 466 20. Greninger AL, Naccache SN, Federman S, Yu G, Mbala P, Bres V, Stryke D, Bouquet J, Somasekar  
467       S, Linnen JM. 2015. Rapid metagenomic identification of viral pathogens in clinical samples by real-  
468       time nanopore sequencing analysis. *Genome Med* 7:99.
- 469 21. Kilianski A, Haas JL, Corriveau EJ, Liem AT, Willis KL, Kadavy DR, Rosenzweig CN, Minot SS.  
470       2015. Bacterial and viral identification and differentiation by amplicon sequencing on the MinION  
471       nanopore sequencer. *Gigascience* 4:12.
- 472 22. Ashton PM, Nair S, Dallman T, Rubino S, Rabsch W, Mwaigwisya S, Wain J, O'grady J. 2015.  
473       MinION nanopore sequencing identifies the position and structure of a bacterial antibiotic resistance  
474       island. *Nat Biotechnol* 33:296.
- 475 23. Lemon JK, Khil PP, Frank KM, Dekker JP. 2017. Rapid nanopore sequencing of plasmids and  
476       resistance gene detection in clinical isolates. *J Clin Microbiol* 55:3530-3543.
- 477 24. Wang J, Moore NE, Deng Y-M, Eccles DA, Hall RJ. 2015. MinION nanopore sequencing of an  
478       influenza genome. *Front Microbiol* 6:766.
- 479 25. Quick J, Loman NJ, Duraffour S, Simpson JT, Severi E, Cowley L, Bore JA, Koundouno R, Dudas G,  
480       Mikhail A. 2016. Real-time, portable genome sequencing for Ebola surveillance. *Nature* 530:228.
- 481 26. Quick J, Grubaugh ND, Pullan ST, Claro IM, Smith AD, Gangavarapu K, Oliveira G, Robles-  
482       Sikisaka R, Rogers TF, Beutler NA. 2017. Multiplex PCR method for MinION and Illumina  
483       sequencing of Zika and other virus genomes directly from clinical samples. *Nat Protoc* 12:1261.
- 484 27. Kim D, Song L, Breitwieser FP, Salzberg SL. 2016. Centrifuge: rapid and sensitive classification of  
485       metagenomic sequences. *Genome Res* 26:1721-1729.
- 486 28. Caporaso JG, Kuczynski J, Stombaugh J, Bittinger K, Bushman FD, Costello EK, Fierer N, Pena AG,  
487       Goodrich JK, Gordon JI. 2010. QIIME allows analysis of high-throughput community sequencing  
488       data. *Nat Methods* 7:335.
- 489 29. Schloss PD, Westcott SL, Ryabin T, Hall JR, Hartmann M, Hollister EB, Lesniewski RA, Oakley  
490       BB, Parks DH, Robinson CJ. 2009. Introducing mothur: open-source, platform-independent,  
491       community-supported software for describing and comparing microbial communities. *Appl Environ*  
492       *Microbiol* 75:7537-7541.
- 493 30. Ip CL, Loose M, Tyson JR, de Cesare M, Brown BL, Jain M, Leggett RM, Eccles DA, Zalunin V,  
494       Urban JM. 2015. MinION Analysis and Reference Consortium: Phase 1 data release and analysis.  
495       F1000Research 4.
- 496 31. Schloss PD, Jenior ML, Koumpouras CC, Westcott SL, Highlander SK. 2016. Sequencing 16S rRNA  
497       gene fragments using the PacBio SMRT DNA sequencing system. *PeerJ* 4:e1869.
- 498 32. Li C, Chng KR, Boey EJH, Ng AHQ, Wilm A, Nagarajan N. 2016. INC-Seq: accurate single  
499       molecule reads using nanopore sequencing. *GigaScience* 5:34.
- 500 33. Alexander D, Swayne D. 1998. Newcastle disease virus and other avian paramyxoviruses, p 156–163.  
501       A laboratory manual for the isolation and identification of avian pathogens 4.
- 502 34. Miller PJ, Dimitrov KM, Williams-Coplin D, Peterson MP, Pantin-Jackwood MJ, Swayne DE, Suarez  
503       DL, Afonso CL. 2015. International biological engagement programs facilitate Newcastle disease  
504       epidemiological studies. *Front Public Health* 3:235.
- 505 35. Afgan E, Baker D, Van den Beek M, Blankenberg D, Bouvier D, Čech M, Chilton J, Clements D,  
506       Coraor N, Eberhard C. 2016. The Galaxy platform for accessible, reproducible and collaborative  
507       biomedical analyses: 2016 update. *Nucleic acids research* 44:W3-W10.
- 508 36. Myers G. Efficient Local Alignment Discovery amongst Noisy Long Reads, p 52-67. *In* (ed),  
509       Springer Berlin Heidelberg,
- 510 37. Katoh K, Misawa K, Kuma Ki, Miyata T. 2002. MAFFT: a novel method for rapid multiple sequence  
511       alignment based on fast Fourier transform. *Nucleic Acids Res* 30:3059-3066.
- 512 38. Li H, Durbin R. 2009. Fast and accurate short read alignment with Burrows–Wheeler transform.  
513       *Bioinformatics* 25:1754-1760.



- 514 39. Li H. 2013. Aligning sequence reads, clone sequences and assembly contigs with BWA-MEM. arXiv  
515 preprint arXiv:13033997.
- 516 40. He Y, Taylor TL, Dimitrov KM, Butt SL, Stanton JB, Goraichuk IV, Fenton H, Poulson R, Zhang J,  
517 Brown CC. 2018. Whole-genome sequencing of genotype VI Newcastle disease viruses from  
518 formalin-fixed paraffin-embedded tissues from wild pigeons reveals continuous evolution and  
519 previously unrecognized genetic diversity in the US. *Virology* 15:9.
- 520 41. Thompson JD, Higgins DG, Gibson TJ. 1994. CLUSTAL W: improving the sensitivity of progressive  
521 multiple sequence alignment through sequence weighting, position-specific gap penalties and weight  
522 matrix choice. *Nucleic Acids Res* 22:4673-4680.
- 523 42. Tamura K, Stecher G, Peterson D, Filipowski A, Kumar S. 2013. MEGA6: molecular evolutionary  
524 genetics analysis version 6.0. *Mol Biol Evol* 30:2725-2729.
- 525 43. Tamura K, Nei M. 1993. Estimation of the number of nucleotide substitutions in the control region of  
526 mitochondrial DNA in humans and chimpanzees. *Mol Biol Evol* 10:512-26.
- 527 44. Tamura K, Nei M, Kumar S. 2004. Prospects for inferring very large phylogenies by using the  
528 neighbor-joining method. *Proc Natl Acad Sci U S A* 101:11030-11035.
- 529 45. Nayak B, Dias FM, Kumar S, Paldurai A, Collins PL, Samal SK. 2012. Avian paramyxovirus  
530 serotypes 2-9 (APMV-2-9) vary in the ability to induce protective immunity in chickens against  
531 challenge with virulent Newcastle disease virus (APMV-1). *Vaccine* 30:2220-2227.
- 532 46. Seal BS, King DJ, Bennett JD. 1995. Characterization of Newcastle disease virus isolates by reverse  
533 transcription PCR coupled to direct nucleotide sequencing and development of sequence database for  
534 pathotype prediction and molecular epidemiological analysis. *J Clin Microbiol* 33:2624-2630.
- 535 47. Seal BS, King DJ, Locke DP, Senne DA, Jackwood MW. 1998. Phylogenetic relationships among  
536 highly virulent Newcastle disease virus isolates obtained from exotic birds and poultry from 1989 to  
537 1996. *J Clin Microbiol* 36:1141-1145.
- 538 48. Sabra M, Dimitrov KM, Goraichuk IV, Wajid A, Sharma P, Williams-Coplin D, Basharat A, Rehmani  
539 SF, Muzyka DV, Miller PJ, Afonso CL. 2017. Phylogenetic assessment reveals continuous evolution  
540 and circulation of pigeon-derived virulent avian avulaviruses 1 in Eastern Europe, Asia, and Africa.  
541 *BMC Vet Res* 13:291.
- 542 49. Rue CA, Susta L, Brown CC, Pasick JM, Swafford SR, Wolf PC, Killian ML, Pedersen JC, Miller PJ,  
543 Afonso CL. 2010. Evolutionary changes affecting rapid identification of 2008 Newcastle disease  
544 viruses isolated from double-crested cormorants. *J Clin Microbiol* 48:2440-2448.
- 545 50. Rehmani SF, Wajid A, Bibi T, Nazir B, Mukhtar N, Hussain A, Lone NA, Yaqub T, Afonso CL.  
546 2015. Presence of Virulent Newcastle Disease Virus in Vaccinated Chickens Farms In Pakistan. *J Clin*  
547 *Microbiol* 53.5:1715-1718.
- 548 51. Wei S, Weiss ZR, Williams Z. 2018. Rapid multiplex small DNA sequencing on the MinION  
549 nanopore sequencing platform. *G3: Genes, Genomes, Genetics*:g3. 200087.2018.
- 550 52. Li H. 2016. Minimap and miniasm: fast mapping and de novo assembly for noisy long sequences.  
551 *Bioinformatics* 32:2103-2110.

552

553 **Figure Legends**

554 **Figure 1.** Schematic diagram of customized Galaxy workflow for MinION sequence data analysis.

555 *Blue shading* indicates pre-processing steps. *Green shading* indicates post-processing steps;  
556 assembly/output is shaded purple. *Purple arrows* indicate different inputs for final consensus  
557 calculation.

558 **Figure 2.** Phylogenetic tree constructed by using the nucleotide sequence (734 bp) of NDV

559 isolates sequenced with MinION, MiSeq and related NDV genotypes from GenBank. The

560 evolutionary histories were inferred by using the maximum-likelihood method based on General

561 Time Reversible model with 500 bootstrap replicates as implemented in MEGA 6. The tree with

562 the highest log likelihood (-9301.9592) is shown. A discrete Gamma distribution was used to

563 model evolutionary rate differences among sites (5 categories [+G, parameter = 0.9325]). The

564 percentages of trees in which the associated sequences clustered together are shown below the

565 branches. The tree is drawn to scale, with branch lengths measured in the number of substitutions

566 per site. The analyses involved 128 nucleotide sequences with a total of 726 positions in the final

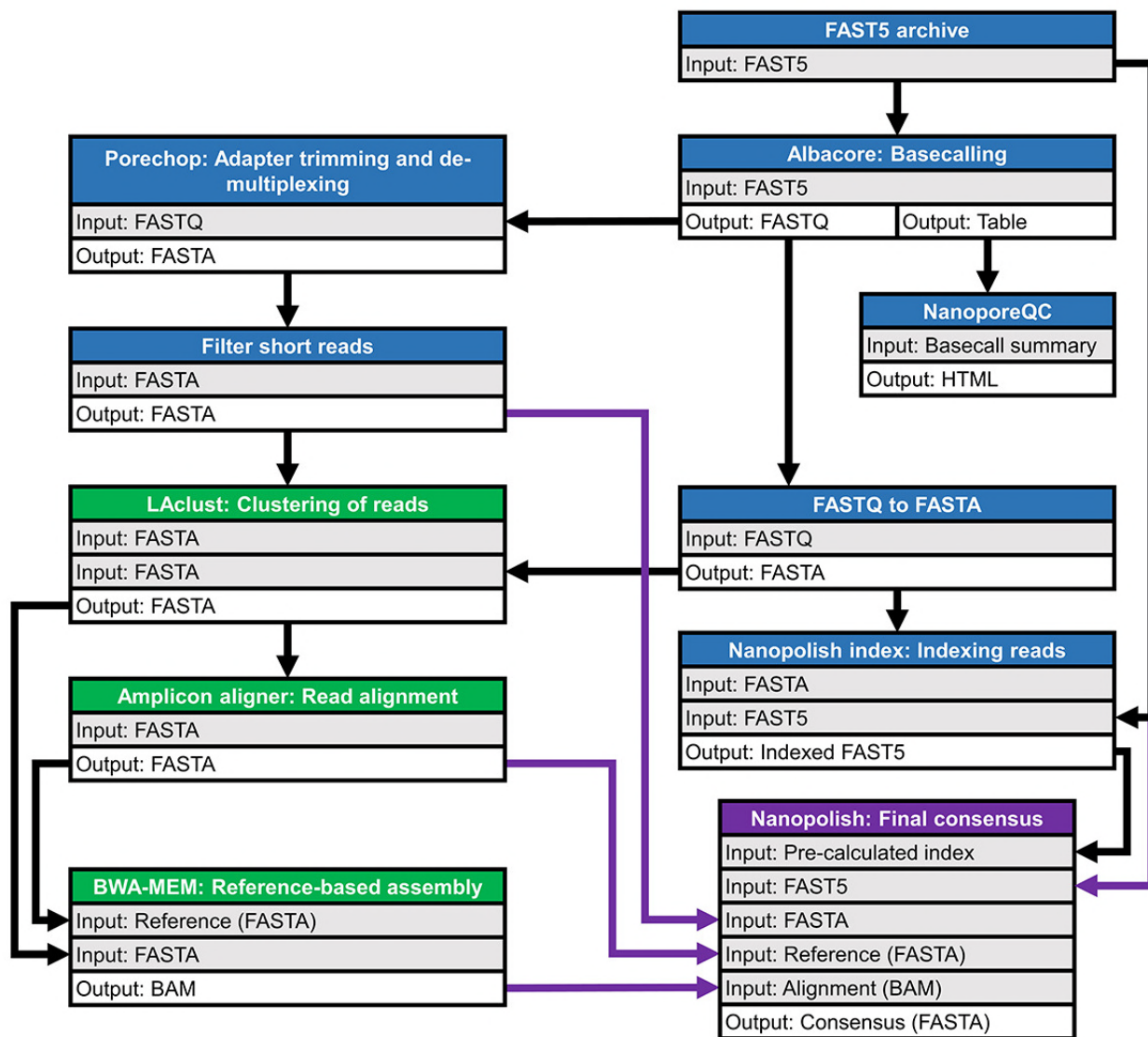
567 datasets. The sequences obtained in the current study are denoted with solid circles in front of the

568 taxa name and bold font. Blue circles indicate isolates from MinION sequencing run 1, green

569 circles indicate isolates from MinION sequencing run 2 and red circles indicate MiSeq sequencing.

570





1  
2 **Figure 1.** Schematic diagram of customized Galaxy workflow for MinION sequence data analysis.  
3 *Blue shading* indicates pre-processing steps. *Green shading* indicates post-processing steps;  
4 assembly/output is shaded purple. *Purple arrows* indicate different inputs for final consensus  
5 calculation.



2 **Figure 2. Phylogenetic tree constructed by using the nucleotide sequence (734 bp) of NDV**  
3 **isolates sequenced with MinION, MiSeq and related NDV genotypes from GenBank.** The  
4 evolutionary histories were inferred by using the maximum-likelihood method based on General  
5 Time Reversible model with 500 bootstrap replicates as implemented in MEGA 6. The tree with  
6 the highest log likelihood (-9301.9592) is shown. A discrete Gamma distribution was used to  
7 model evolutionary rate differences among sites (5 categories [+G, parameter = 0.9325]). The  
8 percentages of trees in which the associated sequences clustered together are shown below the  
9 branches. The tree is drawn to scale, with branch lengths measured in the number of substitutions  
10 per site. The analyses involved 128 nucleotide sequences with a total of 726 positions in the final  
11 datasets. The sequences obtained in the current study are denoted with solid circles in front of the  
12 taxa name and bold font. Blue circles indicate isolates from MinION sequencing run 1, green  
13 circles indicate isolates from MinION sequencing run 2 and red circles indicate MiSeq sequencing.  
14

1 **Table 1.** Comparison of MinION sequencing to RT-qPCR for detection of NDV LaSota

Dilution (EID50/ml)	Total reads	Total NDV reads	Reads per consensus <sup>c</sup>	Percent identity <sup>d</sup>	Consensus length	RT-qPCR <sup>e</sup> (Ct)
	R1 <sup>a</sup>   R2 <sup>b</sup>	R1   R2	R1   R2	R1   R2	R1   R2	R1   R2
10 <sup>6</sup>	6667   11366	6577   10861	200   200	100   100	734   734	21.8, 21.1   22.7, 22.7
10 <sup>5</sup>	4519   6801	4439   6540	200   200	100   100	734   734	26.3, 25.8   26.2, 26.4
10 <sup>4</sup>	3856   8289	3829   7890	200   200	100   100	734   734	28.9, 27.8   29.1, 29.3
10 <sup>3</sup>	164   9484	157   9061	157   200	100   100	734   734	31.4, 31.1   32.7, 32.8
10 <sup>2</sup>	94   4939	85   4725	81   200	100   100	734   734	34.2, 34.8   34.8, 35.3
10 <sup>1</sup>	133   2652	131   2520	73   200	99.04   99.86	729   734	34.9, 34.8   36.9, 36.7

2 <sup>a</sup>Replicate 1

3 <sup>b</sup>Replicate 2

4 <sup>c</sup>*LAclust* was limited (using the available options) to only use 200 reads for downstream analysis

5 <sup>d</sup> Consensus sequence identity to the reference sequence of NDV LaSota sequenced with MiSeq

6 (MH392212/chicken/USA/LaSota/1946)

7 <sup>e</sup>Each dilution performed in duplicate and Ct values from each well are shown here.

8 **Note:** All 60,000 reads obtained during 32 minutes of sequencing run (R1) were utilized for the analysis. All 98,916

9 reads from R2 were utilized for the analysis.

10

1 **Table 2.** Accuracy of consensus sequence identity from 10-fold serial dilutions (EID<sub>50</sub>/ml)  
 2 of NDV LaSota at different time points during MinION sequencing run.

Sequencing run time (min)	Total Raw reads	10 <sup>6</sup>		10 <sup>5</sup>		10 <sup>4</sup>		10 <sup>3</sup>		10 <sup>2</sup>		10 <sup>1</sup>	
		NDV reads <sup>a</sup>	% Identity <sup>b</sup>	NDV reads	% Identity	NDV reads	% Identity	NDV reads	% Identity	NDV reads	% Identity	NDV reads	% Identity
5	4000	283	100	199	100	182	100	10	99.18	2	NA	3	NA
7	8000	644	100	406	100	368	100	14	99.32	8	98.77	5	98.37
10	12000	1029	100	661	100	571	100	23	99.32	16	99.32	8	99.18
12	16000	1397	100	901	100	759	100	29	99.86	17	99.32	14	99.45
14	20000	1772	100	1173	100	1014	100	36	99.73	20	99.45	17	99.59
16	24000	2183	100	1451	100	1231	100	43	99.73	23	99.45	21	99.59
19	28000	2643	100	1775	100	1498	100	56	99.86	29	99.73	25	99.45

3 <sup>a</sup>The numbers represent total number of NDV reads and maximum 200 reads (optional cut-off value) were used to  
 4 generate full length consensus sequence. Minimum 5 reads were used as a cut-off to build consensus sequence.

5 <sup>b</sup>Consensus sequence identity to the reference sequence of NDV LaSota sequenced with MiSeq  
 6 (MH392212/chicken/USA/LaSota/1946)

7 Consensus sequences were BLAST searched against NDV custom database

8 **Note:** Only 28,000 out of total 60,000 reads were utilized for the analysis

- 1 **Table 3.** Detection of NDV and consensus sequence identities of pooled 33 NDV genotypes sequenced with MinION and comparison  
 2 to 23 MiSeq sequences

Sample ID	Input genotype	Output genotype	BLAST search	Consensus length	Alignment length	Number of mismatches	Percentage identity	Number of gaps	Fusion Protein Cleavage site <sup>c</sup>
1	II	II	*MH392212/chicken/USA/LaSota/1946	733	732	0	100	0	low virulent
2	II	II	KJ607167/LHLJ2/goose/2006/China	734	734	0	100	0	low virulent
3	II	II	KJ607167/LHLJ2/goose/2006/China	733	732	0	100	0	low virulent
4	II	II	EU289029/turkey/USA/VG/GA-clone_5/1987	733	734	0	99.86	1	low virulent
5	Ia	Ia	*MH392213/chicken/Australia/Queensland/V-4/10/1966	734	734	0	100	0	low virulent
15	Ia	Ia	MH392213/chicken/Australia/Queensland/V-4/10/1966	734	734	1	99.86	0	low virulent
16 <sup>a</sup>	Ic/VIIId	VIIId	KU295454/chicken/Ukraine/Lyubotyn/961/2003	734	735	3	99.46	1	virulent
17	II	II	*MH392228/poultry/Canada/Ontario/Berwick/853/1948	735	735	0	100	0	virulent
18	II	II	MH392228/poultry/Canada/Ontario/Berwick/853/1948	733	732	12	98.36	0	virulent
19	III	III	*MH392214/chicken/India/Mukteswar/519/1940	734	734	0	100	0	virulent
20	IV	IV	*MH392215/chicken/Nigeria/Kano/1973/N52/899/1973	734	734	1	99.86	0	virulent
21	IV	IV	EU293914/Italy/Italien/1944	734	734	7	99.05	0	virulent
22	XIVb	XIVb	*KT948996/domestic_duck/Nigeria/NG-695/KG.LOM.11-16/2009	734	734	0	100	0	virulent
23	Va	Va	*MH392216/cormorant/USA/MN/92-40140/250/1992	734	734	0	100	0	virulent
24	Vb	Vb	*MH392217/turkey/Belize/4338-4/607/2008	734	734	0	100	0	virulent
25	Vc	Vc	*MH392218/chicken/Mexico/NC/23/686/2011	733	733	2	99.73	0	virulent
26	Vic	Vic	*KY042125/chicken/Bulgaria/Dolno_Linevo/1992	734	734	0	100	0	virulent
27	VIm	VIm	*KX236101/pigeon/Pakistan/Lahore/25A/2015	734	734	0	100	0	virulent
28	VIIj	VIIj	*MH392219/chicken/Egypt/Sohag/18/1020/2014	734	734	0	100	0	virulent
29	VIIe	VIIe	KJ782375/goose/China/GD-QY/1997	734	734	16	97.82	0	virulent
30	VIIIi	VIIIi	*KX496962/wild_pigeon/Pakistan/Lahore/20A/996//2015	734	734	0	100	0	virulent
31	IX	IX	*MH392220/poultry/China/04-23/C12/647/2004	734	734	0	100	0	virulent
32	IX	IX	MH392220/poultry/China/04-23/C12/647/2004	734	734	1	99.86	0	virulent
33	Xb	Xb	*MH392221/mallard/USA/MN/99-376/163/1999	734	734	0	100	0	low virulent
34	Xa	Xa	*GQ288378/northern_pintail/USA/OH/87-486/1987	734	734	0	100	0	low virulent
35	XIIa	XIIa	*JN800306/poultry/Peru/1918-03/2008	734	734	0	100	0	virulent
36	XIIIb	XIIIb	*MH392222/chicken/Pakistan/SPVC/Karachi/27/558/2007	734	734	6	99.18	0	virulent
37 <sup>b</sup>	Vic/XIIIb	XIIIb	*MH392223/chicken/Pakistan/SPVC/Karachi/33/556-XIII/2007	731	734	1	99.46	3	virulent
38	XIVb	XIVb	*MH392225/chicken/Nigeria/KD/TW/03T/N45/720/2009	734	734	0	100	0	virulent
39	XVI	XVI	*MH392226/chicken/Dominican_Republic/FO/499-31/505/2008	734	734	0	100	0	virulent
40	XVIIa	XVIIa	*KY171995/VRD124/06/N11/867/chicken/2006/Nigeria	734	734	0	100	0	virulent
41	XVII	XVII	*KU058680/903/domestic_duck/Nigeria/KUDU-113/1992	734	734	0	100	0	virulent
42	XVIIIb	XVIIIb	*MH392227/chicken/Nigeria/OOT/4/1/N69/914/2009	734	734	0	100	0	virulent

3 <sup>a</sup>Sample #16 was tested by two, genotype-specific PCRs followed by Sanger sequencing

4 <sup>b</sup>Sample #37 was also sequenced on Illumina Miseq to detect mixed NDV infections

- 5 °F protein cleavage sites of virulent NDV genotypes contains more than 3 basic amino acids [(112(R/K)N<sup>o</sup>t<sup>e</sup>-R-(Q/K/R)-(R/K)-R-F117)] and low virulent NDV
- 6 genotypes has monobasic amino acids [(112(G/E)-(R/K)-Q-(G/E)-R-L117)]
- 7 \*Same isolate was also sequenced with Miseq
- 8 **Note:** Isolates known to have low virulence are highlighted in bold.

1 **Table 4.** Identification and virulence prediction of NDV genotypes in clinical swab samples collected during disease outbreaks in 2015.

Sample ID	Miseq genotypes	MinION genotypes	ID of the MinION hit	Reads per cluster	Consensus length	Percentage identity	Fusion protein cleavage site
44	VIII	VIII	chicken/Pakistan/Wadana_Kasur/PNI_PF_(14F)/2015	200	734	100	virulent
45	VIII	VIII	chicken/Pakistan/Wadana_Kasur/PNI_PF_(14F)/2015	28	734	99.31	virulent
	<b>II</b>	<b>II</b>	<b>chicken/USA/LaSota/1946</b>	<b>5</b>	<b>733</b>	<b>96.44</b>	<b>low virulent</b>
46	VIII	VIII	chicken/Pakistan/Wadana_Kasur/PNI_PF_(14F)/2015	10	733	99.13	virulent
	<b>II</b>	<b>II</b>	<b>chicken/USA/LaSota/1946</b>	17	733	<b>98.51</b>	<b>low virulent</b>
47	VIII	ND <sup>d</sup>	NA <sup>e</sup>	NA	NA	NA	NA
	<b>II</b>	<b>II</b>	<b>chicken/USA/LaSota/1946</b>	<b>139</b>	<b>732</b>	<b>99.32</b>	<b>low virulent</b>
48	<b>ND</b>	<b>II</b>	<b>chicken/USA/LaSota/1946</b>	<b>200</b>	<b>732</b>	<b>99.59</b>	<b>low virulent</b>
	VIII	VIII	chicken/Pakistan/Wadana_Kasur/PNI_PF_(14F)v/2015	21	733	99.13	virulent
49	VIII	ND	ND	ND	ND	ND	ND
	<b>II</b>	<b>II</b>	<b>chicken/USA/LaSota/1946</b>	<b>200</b>	<b>732</b>	<b>99.32</b>	<b>low virulent</b>
50	VIII	VIII	chicken/Pakistan/Wadana_Kasur/PNI_PF_(14F)/2015	113	734	100	virulent
51	VIII	VIII	chicken/Pakistan/Mirpur_Khas/3EOS/2015	200	734	100	virulent
52 <sup>a</sup>	VIII	ND	NA	NA	NA	NA	NA
53	VIII	VIII	exotic Parakeets/Pakistan/Charah/Pk29/29A/2015	5	726	98.5	virulent
54	NO NDV	ND	NA	NA	NA	NA	NA
55	NO NDV	ND	NA	NA	NA	NA	NA
56	NO NDV	ND	NA	NA	NA	NA	NA
57	NO NDV	ND	NA	NA	NA	NA	NA
58	VIII	VIII	chicken/Pakistan/Gharoo/Three_star_PF_(7G)/2015	8	729	99.32	virulent
TN <sup>b</sup>	NA	ND	NA	NA	NA	NA	NA
EN <sup>c</sup>	NA	ND	NA	NA	NA	NA	NA

2 <sup>a</sup> After bead purification, the barcoded amplicon concentration of this sample was lowest in this pool.

3 <sup>b</sup> Template control negative

4 <sup>c</sup> Negative extraction control

5 <sup>d</sup>Not detected

6 <sup>e</sup>Not applicable

7 **Note:** Isolates known to have low virulence are highlighted in bold.